

CHAPTER THREE

Introduction to Two Practical Laser Systems

3

Introduction to Two Practical Laser Systems

3.1 Introduction

To give a little more practical emphasis to some of the ideas we have dealt with so far, let us consider some of the details of two real systems where population inversion and laser oscillation can be obtained. One of these lasers uses an amplifying medium that is a crystalline solid, the other a gas. In each case, the amplifying medium is pumped into a state of population inversion by feeding energy into it in an appropriate way. Laser oscillation occurs when the amplifying medium is placed between a pair of suitable aligned mirrors that provide the necessary optical feedback to cause oscillation to occur. The first of these two systems is the ruby laser. This was the first laser, originally made to work in July 1960 by Theodore Maiman of the Hughes Aircraft Company in Malibu, California.

3.2 The Ruby Laser

The amplifying medium of this laser is crystalline aluminum oxide (sapphire) doped with Cr^{3+} ions, typically in concentrations of about 0.05% by weight. The crystal structure of the undoped sapphire is shown in Fig. (3.1). When the crystal is doped with Cr^{3+} ions some of the aluminum sites become occupied by chromium. It is these Cr^{3+} ions that are the active particles in the amplification process. A schematic energy

Fig. 3.1.

level diagram for the Cr^{3+} ions in such material is shown in Fig. (3.2). Population inversion is produced by irradiating such a ruby crystal with light that causes absorption transitions from the ground state into the broad absorption bands labelled 4F_1 and 4F_2 . The absorption spectrum of a typical ruby laser crystal is shown in Fig. (3.3), which clearly shows these two broad absorption bands, one in the violet–blue and the other in the green–yellow region, that lead to the 4F levels. These absorption bands are very broad because the very many sub-levels of the 4F levels of slightly different energy are “smeared” together by line broadening. The sharper absorption peak due to the laser transition itself is also visible as a small peak around 700 nm in Fig. (3.3). Fig. (3.4) shows a more detailed absorption spectrum of the laser transition that illustrates that the laser transition consists of two closely spaced lines, labelled R_2 and R_1 . In both Figs. (3.3) and (3.4) the amount of absorption is seen to depend on the relative linear polarization of the incident light and the orientation of the crystal.[†]

The 4F_1 and 4F_2 levels decay (with lifetimes ~ 50 ns) preferentially into the upper laser level 2E . This level actually consists of a pair of closely spaced levels separated by 29 cm^{-1} .[‡]

The splitting of this energy level arises because of the symmetry of the

[†] A fuller discussion of the effect of crystal symmetry on the propagation of light is given in Chapter 18.

[‡] The unit cm^{-1} is frequently used as a unit of energy. If two energy levels are 1 cm^{-1} apart, this implies that the wavelength of the transition between them is 1 cm, and its frequency is 3×10^{10} Hz i.e.,

$$\Delta E = h\nu = \frac{hc}{\lambda} = 3 \times 10^{10} h.$$

Fig. 3.2.

Fig. 3.3.

Fig. 3.4.

If two levels are $k \text{ cm}^{-1}$ apart, then

$$\Delta E = \frac{hc}{\lambda} = \frac{hc}{1/k} = (k \times 3 \times 10^{10})h.$$

crystal lattice. The Cr^{3+} ions in the aluminum oxide lattice have energy levels which are affected by the spatial arrangement of aluminum and oxygen ions around them. If this arrangement had exact octahedral symmetry around each Cr^{3+} ion no splitting would occur. In practice the symmetry of the arrangement is rhombohedral and the small energy splitting results.

In practice, to produce a state of population inversion in the crystal, it is necessary to irradiate the crystal with a very intense light source. This is most easily accomplished with a flashlamp, which uses a tube, generally made of quartz and filled with a noble gas, through which energy stored in a capacitor charged to high voltage is discharged. Such a lamp can, for the short period of time during which current flows through it, produce a very high light intensity. A simple electrical circuit for the operation of such a lamp is shown in Fig. (3.5). The spectral characteristics of the lamp will depend on a number of parameters: for example, capacitor size, voltage, tube diameter, the filling gas and its pressure. Generally if the discharge is of short duration $\lesssim 10 \mu\text{s}$ and high energy, the hot gas in the lamp will emit approximately as a black body, perhaps at an effective temperature of 20,000 K, where much of its emission would be in the blue and ultraviolet. For ruby laser excitation the emission of the lamp is optimized in the region of the crystal's absorption bands by using slower flashlamp pulses (100 μs –10 ms) and appropriate gas mixtures. If the flashlamp intensity is great enough, then sufficient ground state ${}^4A_2 \text{Cr}^{3+}$ ions can be excited to the $2\bar{A}$ and \bar{E} levels via the broad absorption bands 4F_2 and 4F_1 that a population inversion exists between the $2\bar{A}$ and \bar{E} levels and the split ground state. An efficient transfer occurs from the broad absorption bands to these upper laser levels because the radiative decay from these bands to the ground state has a lifetime of about 3 μs , against a value of about 50 ns into the upper laser levels. Consequently, about 99% of the ions that reach these bands transfer into the upper laser levels. These levels have an overall lifetime $\tau_2 \simeq 3 \text{ ms}$ and lose their energy almost exclusively by spontaneous emission to the ground state so that $A_{21} \simeq 1/\tau_2$. Because these levels are relatively long lived, if the exciting flash is shorter than their overall lifetime then most of the ions transferred into them will still be there when the flash is finished. The main laser transition that occurs is R_1 , between level \bar{E} and the ground state, its wavelength is 694.3 nm (a visible dark red color). Laser oscillation can also be obtained on the transition R_2 , but only by taking special measures to reduce the gain of R_1 , which otherwise operates preferentially.

Fig. 3.5.

Fig. 3.6.

Because of the arrangement of its energy levels and the way it is excited, the ruby laser falls into the class of what are called three-level lasers. Most efficient lasers fall into the class of four-level lasers (two-level lasers are also possible). The difference between three- and four-level systems is best illustrated with reference to the schematic energy level diagram in Fig. (3.6). If $E_1 \ll kT$ the system is a three-level laser system, if $E_1 \gg kT$ it is a four-level system. Since in the ruby laser $E_1 \sim 0$, it is a three-level laser. We shall see later that it is intrinsically more difficult to obtain population inversion in a three- rather than a four-level system. With this fact in mind it is perhaps surprising that the first operational laser was of the three-level type.

Typical ruby lasers employ cylindrical crystals 1–20 mm in diameter, 20–200 mm in length. Usually the resonant cavity consists of the parallel polished faces of the crystal, one of which is coated to make it 100% reflecting. The Fresnel reflection from the other end is often sufficient to provide the optical feedback necessary for oscillation, although it may

Fig. 3.7.

be made to have a higher reflection coefficient by giving it a suitable coating. Theodore Maiman's original ruby laser employed a very small crystal surrounded by a helical flashlamp, the whole being contained inside a coaxial cylindrical metal reflector, as shown in Fig. (3.7)^[3.4]. In this arrangement the optical pumping of the laser is axisymmetric, which offers certain advantages in many applications, since the population inversion produced in the crystal is then itself axisymmetric. Prior to obtaining laser oscillation in the ruby system, Maiman and his colleagues had measured the absorption spectrum and the relative decay rate of the important energy levels^[3.3]. It was these measurements which made them believe that it would be possible to obtain population inversion in the ruby system.[†]

Although helical flashlamp excitation is still sometimes used, other methods of optical pumping are more common. The most usual arrangement employs a cylindrical flashlamp and crystal placed along the two focal lines of an elliptical reflector, as shown in Fig. (3.8). It is a property of such an elliptical reflector that rays of light from one focus, after reflection, pass through the other focus. Thus, light from the flashlamp is efficiently reflected towards the laser crystal.

3.3 The Helium–Neon Laser

The helium–neon laser was the first gas laser to be operated, and also

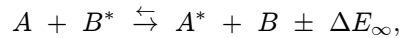
[†] Surprisingly enough, when the first observations of laser action were made and Maiman submitted the article describing the results to *Physical Review Letters*, his article was rejected. Consequently, the first article describing successful operation of a laser appeared in the periodical *Nature*.

Fig. 3.8.

Fig. 3.9.

the first CW (continuous wave) laser. The production of a population inversion in this system occurs as a result of energy transfer processes between metastable helium atoms and ground state neon atoms, which are as a result excited to various upper laser levels.

In a collisional excitation transfer process of the kind



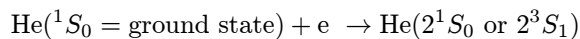
where the colliding particles are not molecular and an asterisk indicates that the particle is in an excited state, the probability of the reaction occurring becomes extremely small if the energy discrepancy ΔE_∞ of the reaction exceeds kT ^[3.5], as shown in Fig. (3.9). ΔE_∞ is the energy difference between the excited states A^* and B^* at large (theoretically infinite) separation of the reacting particles (ΔE is a function of the separation of the two atoms in an A^* and a B state respectively because of forces between them; the effect of this force goes to zero as the two atoms become infinitely far apart).

If either of the colliding particles is molecular, then the probability

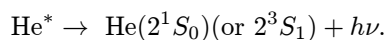
Fig. 3.10.

of reaction can remain large even if ΔE_∞ exceeds kT , since one or the other of the particles may be able to release or store energy in internal degrees of freedom, such as vibration.

In the helium-neon laser the excitation transfer processes occur in a glow discharge in a helium-neon mixture at a total pressure of about 1 torr.[†] The mixture is usually in the range 5:1–10:1 helium to neon. The discharge is produced either by DC or RF excitation in tubes usually of 1–20 mm inside diameter, and carries a current density from 0.1 to 1 A cm⁻². By various collisional and radiative processes electrons excite ground state helium atoms to the metastable 2^1S_0 and 2^3S_1 levels, as shown in Fig. (3.10)



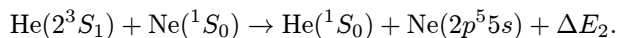
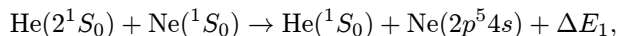
or



As the 2^1S_0 and 2^3S_1 states are metastable they do not lose energy readily by undergoing spontaneous emission (the radiative lifetime of the 2^3S_1 state is well in excess of one hour). However, these metastable states can lose energy in collisions, and in collisions with ground state neon atoms high probabilities exist for energy transfer in reactions such

[†] The torr, named for the seventeenth century Italian mathematician Torricelli, who invented the mercury manometer, is a unit of pressure equal to 1 mm of mercury. Standard atmospheric pressure is 760 torr. 1 torr \equiv 133 Pascal (1 Pa \equiv 1 N m⁻²).

as



The energy discrepancies ΔE_1 , ΔE_2 are small, ΔE_1 is $\sim 400 \text{ cm}^{-1}$, comparable with, or less than kT for the hot atoms in the discharge. The neon $4s$ and $5s$ levels that are excited in this way, under appropriate conditions, exhibit population inversion with respect to the $3p$ and $4p$ levels. The existence of such a population inversion does, however, require that the lower laser levels not be efficiently populated. This could occur either because they are excited by electron collisions or because population builds up in them if they become long lived.

One interesting laser transition that results because of population inversion is between one of the $4s$ and one of the $3p$ levels and occurs at $1.15 \mu\text{m}$. This transition (in the near-infrared and consequently invisible to the human eye) was the first transition to be observed in the He-Ne laser. When Javan, Bennett, and Herriott first obtained oscillation on the $1.15 \mu\text{m}$ transition in 1961^[3,6], their success was essentially a result of investigating a system where, theoretically, solid evidence existed for the possible obtainment of a population inversion. Their laser, the first CW and gas laser is shown in Fig. (3.11). Many of the features of this system are of interest, particularly since most of the technological features of the device have been superseded in more recent He-Ne gas lasers. The glow discharge was produced in this first gas laser by coupling RF power to the tube with external electrodes: in most modern CW gas lasers direct DC input to the gas is preferred. The laser mirrors situated at each end of the amplifier tube were plane, and were fixed inside metal assemblies to allow them to be aligned parallel while retaining the vacuum integrity of the structure. Nowadays, Brewster angle window assemblies allow the laser mirrors to be situated outside the tube. Such windows allow a plane-polarized laser oscillation to occur without the Fresnel reflection loss normally associated with in-cavity windows. It also turns out that plane parallel mirror resonators are extremely sensitive to misalignment (misalignment of a few seconds of arc will prevent oscillation being obtained). In order to be sure that their laser mirrors would be aligned, Javan and his coworkers fixed one mirror to an electromechanical device that wobbled the mirror through a range of angular positions near the expected position where parallelism with the other mirror would occur. By using an image converter tube, which made the infrared laser beam visible, they were able to detect

Fig. 3.11.

Fig. 3.12.

the burst of oscillation as the laser mirror passed through the alignment position. It was subsequently discovered that the use of spherical mirrors of appropriate radius of curvature made the alignment tolerances of the cavity much less severe (oscillation could be sustained over perhaps a $\frac{1}{2}$ degree range near the coaxial position). A schematic diagram of a gas laser system with DC excitation, Brewster windows and external spherical mirrors is shown in Fig. (3.12).

The $1.15\ \mu\text{m}$ transition first observed in the helium–neon laser is now mainly of historical importance. Many other laser transitions between the $(5s, 4s)$ and $(4p, 3p)$, levels have been observed since, the most important of which are between the $5s$ and $3p$ and the $5s$ and $4p$ levels. Two of these transitions are particularly noteworthy, those at $632.8\ \text{nm}$ and $3.39\ \mu\text{m}$. The red laser transition at $632.8\ \text{nm}$ is the one most familiar to anyone who has ever seen one of the many thousands of commercial helium–neon lasers which are in widespread use. Population inversion on this transition results from the energy transfer pumping from helium 2^1S

metastables. The lower level of the transition has a radiative lifetime of about 10 ns, about a factor of ten times shorter than that of the upper level. The desirability of such a favorable lifetime ratio in a laser system will become more apparent later. It can be seen from Fig. (3.10) that the lower level of the 632.8 nm decays to one of the $3s$ levels. This level is metastable and loses its energy mostly in collisions with the discharge tube walls. If the population of this level rises too high, repopulation of the lower laser level from it may destroy the population inversion. This repopulation may result from electron collisional excitation of the $3p$ levels from the $3s$ levels, or by the reabsorption of photons emitted by atoms in the lower laser level (this latter phenomenon is called *radiation trapping*^{[3.7],[3.8]}). If the rate of collisional deactivation of the $3s$ levels is increased, for example, by reducing the diameter of the laser tube, then the gain of the 632.8 nm transition (and also the 1.15 μm transition) is increased. The gain increases inversely with tube diameter, but cannot be increased too far by this means or the available volume of inverted gas falls, diffraction losses increase, and the laser's power output decreases.

The 3.39 μm laser transition shares a common upper level with the 632.8 μm transition but has a very much higher small-signal gain (as high as 50 dB m^{-1}). This high gain is partly due to a very favorable lifetime ratio for the 3.39 μm transition and also to its longer wavelength. In gas lasers of this kind the gain is proportional to at least λ^2 (λ^3 if the transition is predominantly Doppler-broadened). Because of its higher gain the 3.39 μm transition has a lower oscillation threshold under conditions of comparable feedback than the 632.8 nm transition. Under such conditions it will oscillate preferentially and prevent oscillation at 632.8 nm. This occurs because it builds up in oscillation first and "clamps" the population inversion (because of gain saturation) at a threshold level for its oscillation. This will be discussed in more detail in Chapter 5. The population inversion may be clamped at a level too low for laser oscillation at 632.8 nm. To prevent this occurring, the oscillation threshold at 3.39 μm must be raised. In short lasers with quartz or glass windows these windows introduce sufficient loss for this to occur, also the resonator mirrors will generally have lower reflectivity at 3.39 μm than at 632.8 nm. In long helium–neon lasers ($\gtrsim 1$ m) the loss introduced by the windows and mirrors may not prevent parasitic oscillation at 3.39 μm . There are two common ways to lower the gain at 3.39 μm in such lasers. An in-cavity methane cell (which absorbs 3.39 μm strongly but not 632.8 nm) can be used or a spatially inhomogeneous magnetic

field can be applied to the discharge tube. Such a field introduces a Zeeman splitting[†] of the $3.39\ \mu\text{m}$ laser transition that is different at different points along the discharge: this effectively increases the linewidth of the laser transition and reduces its gain. The effect of the magnetic field is much smaller at $632.8\ \text{nm}$ because its Doppler-broadened linewidth is already large. The spatially inhomogeneous magnetic field can be supplied by a series of bar magnets placed outside the tube and spaced along its length.

[†] An effect where a magnetic field separates an energy level into a series of closely-spaced sub-levels of slightly different energy. The transition changes from a single transition at a unique center frequency to a group of closely-spaced transitions at center frequencies that depend on the strength of the applied magnetic field.

References

- [3.1] V. Evtuhov and J.K. Neeland, "Pulsed ruby lasers," in *Laser: A Series of Advances*, Vol. I, A.K. Levine, Ed., Marcel Dekker, New York, 1966.
- [3.2] T.H. Maiman, R.H. Hoskins, I.J. D'Haenens, C.K. Asawa, and V. Evtuhov, "Stimulated emission in fluorescent solids II spectroscopy and stimulated emission in ruby," *Phys. Rev.* **123**, 1151–1157, 1961.
- [3.3] D.C. Cronmeyer, "Optical absorption characteristics of pink ruby," *J. Opt. Soc. Am.* **56**, 1703–1706, 1966.
- [3.4] T.H. Maiman, "Stimulated optical radiation in ruby," *Nature*, **187**, 493–494, 1960.
- [3.5] N.F. Mott and H.S.W. Massey, *The Theory of Atomic Collisions*, Oxford University Press, Oxford, 1965.
- [3.6] A. Javan, W.R. Bennett, Jr., and D.R. Herriott, "Population inversion and continuous optical maser oscillation in a gas discharge containing a He-Ne mixture," *Phys. Rev. Lett.*, **6**, 106–110, 1961.
- [3.7] T. Holstein, "Imprisonment of resonance radiation in gases," *Phys. Rev.*, **72**, 1212–1233, 1947.
- [3.8] T. Holstein, "Imprisonment of resonance radiation in gases II," *Phys. Rev.*, **83**, 1159–1168, 1951.